Journal of Information & Optimization Sciences
ISSN 0252-2667 (Print), ISSN 2169-0103 (Online)
Vol. 47 (2026), No. 1, pp. 145–165
DOI : 10.47974/JIOS-1505

A projectile model for pandemics : Application to early transmission and control of COVID-19 in countries and the China example

Okecukwu K Nwofor *
Department of Physics
Imo State University
PMB 2000
Owerri
Nigeria

Chioma N Nwofor #
Department of Microbiology
Imo State University
PMB 2000
Owerri
Nigeria

Nathaniel E. Onyenwe $
Department of Pharmaceutical Microbiology
Igbinedion University Okada
Nigeria

Abstract

We introduce a projectile model for pandemics which shows that a pandemic without control spreads in log-time scale within a population in the form of a mechanical projectile in a free atmosphere. Hence, a controlled pandemic behaves like a "decayed" projectile motion in a resistive atmosphere. If β is the "decay polynomial" associated with the decay in amplitude and range of a projectile in a resistive atmosphere, then *U* by analogy will be the "control polynomial" associated with the reduction in intensity and duration of a pandemic due to control measures. By comparing the r-square of the best-fit polynomial to β (i.e R_β^2) to the r-square of the same-degree best-fit polynomial to *U* (i.e R_μ^2), the parameter; $\epsilon = R_\beta^2/R_\mu^2$ serves the purpose of assessing pandemic control levels for different populations. The above framework was used to assess early transmission and control of COVID-19 in 20 high-burden

* *E-mail:* **okeynwofor@yahoo.com (Corresponding Author)**
# *E-mail:* **chiomanwofor@gmail.com**
$ *E-mail:* **o_nathejik@yahoo.com**

countries from World Health Organization (WHO) COVID-19 case trends within the first half of year 2020. Four clusters were segregated using the ϵ parameter. China and countries from Europe and North America, appeared in Cluster 1- with the most effective early COVID-19 control, while countries with less effective control mainly from Africa (although with the least transmission), Asia and South America appeared in Clusters 2, 3 and 4. The framework achieves the purpose of obtaining an objective metric for pandemic control assessment; hence China with $\epsilon = 1.1$ showed a near projectile-type controlled transmission so that the measures adopted by China may serve as model for future pandemic control especially in Africa where poor medical and social infrastructure was evident in the poor handling of the pandemic.

Subject Classification: *92B99.*

Keywords: *Projectile model for pandemics, Pandemic transmission, COVID-19, COVID-19 control, Mechanical projectile, Non-pharmaceutical measures.*

1. Introduction

The emergence of the novel strain of the Severe Acute Respiratory Syndrome-Coronavirus-2 (SARS-CoV-2) in Wuhan city in China in the later period of 2019 resulted in the declaration by the World Health Organization (WHO) of the global pandemic known as COVID-19 with early average case fatality rate of 2.2% ([1][2]). In the initial outbreak and with the absence of regular therapeutic cure and vaccines, non-pharmaceutical control measures remained the best option for reducing the disease burden. Following the major disease transmission routes for COVID-19 which are droplet transmission from person to person, aerosols from respiratory droplets mixing with air and contamination of surfaces by droplets ([3],[4],[5]), the recommended control measures included physical and social distancing, constant washing of hands with soap under running water for at least 20 seconds and application of hand sanitizers containing at least 60% alcohol ([6]). Different countries instituted these control measures with different levels of success. The most far-reaching measures taken by most countries with various degrees of case records were the partial or total *lock-down* of the population and contact tracing and isolation of infected persons while symptomatic patients were given supportive care ([6][7]). Whereas many countries, initiated lock-down rapidly and comprehensively, especially at the epicenters of the pandemic, many others did not: especially in the developing world such as Africa where lock-down measures were seen to seriously compromise livelihoods of the highly vulnerable populace.

Although a good number of vaccines have now been produced to combat the pandemic, the global roll out is still inadequate especially in the developing world such as Africa. The pandemic consequently raged on in successive waves in many countries with associated mutations into new more transmissible strains ([8]). As COVID-19 may not be the last global pandemic, it is obvious that the Non-Pharmaceutical Interventions (NPIs) which characterized the early management of the pandemic will still offer the most effective control of pandemics in the future. Evaluating how various countries faired in their control of the pandemic in the early period is crucial for countries to make inferences regarding the effects of the steps they took to stem the pandemic and by so doing take steps in building capacity for quickly responding to and managing future pandemics ([9]). These are of particular relevance for countries with poor medical and social infrastructure as shown by Singh and co-workers ([10]) and these are mostly found in Africa.

Some comprehensive evaluations of country-response to pandemics especially the COVID-19 have been undertaken (e.g, [11]). Other notable appraisals include the analysis of some demographic aspects of the disease transmission in parts of India by Bhatnagar and co-workers ([12]). and the work by Jamison and co-workers ([13])., which generated performance ranking for 35 countries based on doubling-times of cases and deaths at days 25, 65 and 135, while Mariano and Ozmucur ([9]) used both health and economic disaster indicators to assess country-performance. Graph modeling was also used in determining the best strategies for mitigating the impact of pandemics such as COVID-19 (e.g. [14]).). In this work, we propose a framework that utilizes the analogy between mechanical projectiles in both free and resistive atmosphere and the probability density functions of a pandemic transmission (e.g. COVID-19) without and under control respectively. The framework is used to derive equations and parameters for objective assessments of the level of COVID-19 control. In Section 2, we present the background and mathematical formulation of the framework and thereafter in Section 3 we set up the parameters used in assessing the level of control of COVID-19 spread achieved by 20 selected countries in their various “early waves”. The summary of the results obtained is presented in Section 4. The implications of the results in deriving benchmarks for future management of pandemics in countries especially in Africa are discussed in Section 5, while the summary and conclusions are provided in Section 6.

2.0 A Projectile Model for Pandemics

2.1 *Preamble*

The underlying assumptions of the projectile analogy for pandemics (PMP) introduced in this work is implied in the pandemic pathway popularized by the classical "SIR" model ([15]). which requires that the population exposed to a pandemic is "susceptible" on account of the predominance of "infectibles" who continuously infect more people in the population. Hence in the unlikely situation where communities do nothing in the face of the pandemic, the number of new infections grows exponentially under a close-population assumption (see[16]). The exponential growth situation would persist until at such a time when the disease "removes" much of the population through death or loses its potency along the transmission chain due to "infected" people developing immunity. This rapid exponential pattern of the business-as-usual scenario is a Gaussian distribution over a full pandemic cycle which produces a parabola in log time-scale just like a mechanical projectile. Since a naturally transmitting pandemic results in severe depletion of the population, artificial control measures such as lock-down, social distancing, use of face masks and personal hygiene, are therefore initiated to flatten the exponential curve. This action is analogous to the dampened motion of a projectile in a resistive atmosphere. The PMP framework therefore requires a comparison between the transmissions of a pandemic with and without control and the motions of a mechanical projectile in free and resistive atmosphere respectively as a way of learning how well the pandemic is controlled. The mathematical basis of this framework is set up in the following sub-section.

2.2 *Mathematical Formulations*

The path of a projectile in an atmosphere without resistance is shown in Figure 1. It is a two-dimensional motion at constant acceleration equivalent to two independent motions in the x and y directions. These two motions can be incorporated in a vector representation so that the position vector of the projectile traveling close to the earth with velocity $\overline{v}_i$ after a time t is;

$$\overline{r}_j = \overline{r}_i + \overline{v}_i t + \frac{1}{2}\overline{g}\, t^2 \quad (1)$$

Where $\overline{r}_i = x_i + y_i$ is the initial position of the particle and $g \sim 9.81\text{ms}^{-2}$ is the gravitational acceleration.

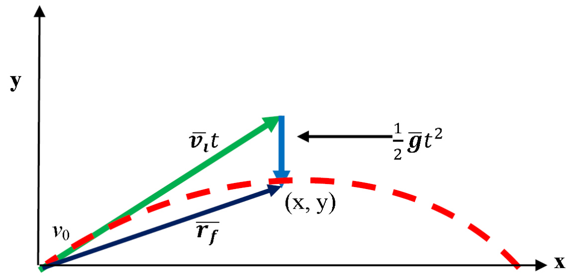

Figure 1

Schematic of projectile motion in free atmosphere

Since the motion of the projectile is initiated by the velocity, $\overline{v}_i$ the linear term of the motion is given by; $\overline{v}_i t$ while the curvature term which has the effect of reducing the range is given by, $\frac{1}{2}\overline{g}t^2$.

We need to establish how the projectile fits the pandemic transmission. We proceed as follows: Let the cases of infection in a closed-population pandemic space z be $C(z)$. This can be represented by the standard *Gaussian* of the form;

$$C(z) = \int_{-\infty}^{z} P \exp\left[-\frac{1}{2}z^2\right] dz \tag{2}$$

Where $P = \frac{1}{\sigma\sqrt{2\pi}}$ is the amplitude of the normalized distribution of the random variable $z = \frac{t-\overline{t}}{\sigma}$ of mean = $\overline{t}$ and standard deviation = σ.

In log time-scale, the transmission vector $T(z)$, following equation 2 has the approximate form;

$$T(z) = In\, C(z) \approx -z^2 \tag{3}$$

Hence in the absence of lockdown and other control measures, the pandemic curve follows a cumulative distribution pattern that is quadratic in log time-scale. The standard form of the transmission $(T(z)$ is:

$$T(z) = \eta_0 + \eta_1 z + \eta_2 z^2 \tag{4}$$

And this has the same form as equation 1 with the more general form being:

$$T(z) \approx \eta_0 + \eta_1 z + \eta_2 z^2 + \ldots + \eta_N z^N$$

Where η_N for each η are appropriate coefficients.

Table 1

The projectile model of pandemic (PMP) Framework

Equation	Measured quantity	Linear term	Quadratic term	Decay/control c
$\overline{r}_f = \overline{r}_i + v\,t$ $\overline{v}_i t + \frac{1}{2}\overline{g}t^2$	$\overline{r}_f$ $\overline{g}t$ (Signifying motion)	$\overline{v}_i t$ Governing parameter: velocity (v_i)	$\frac{1}{2}\overline{g}t^2$ Dissipation of linear motion towards curved motion- Governing parameter: gravity (**g**) (influenced by earth's shape and mass)	Resistance (e.g. friction of air molecules- causing increased curvature)
$T(z) = \eta_0 + \eta_1 z + \eta_2 z^2$	$T(t)$ (Signifying transmission or spread)	$\eta_1 z$ *Governing parameter: transmissivity* (η_1)	$\eta_2 z^2$ *Flattening of pandemic transmission. Governing parameter: curvature coefficient* (η_2) *(influenced by population demography and immunity)*	Control Measures (e.g. lock-down, social distancing, use of face masks, personal hygiene- causing increased curvature)

Hence by comparing equations 1 and 4, the *analogy between the mechanical projectile motion and the pandemic transmission is obvious from the mapping;*

$$\overline{r}_j \to T(z); \overline{r}_i \to \eta_0;\ \overline{v}_i \to \eta_1;\ \tfrac{1}{2}\overline{g} \to \eta_2; \tag{6}$$

The projectile analogy of pandemics framework is conceptualized in Table 1.

In Table 1, the first-order term of (5) (η_1), provides a linear approximation to the efficiency of pandemic transmission (i.e **transmissivity**). On the other hand, the quadratic term (η_2), appropriately models the **curvature** (κ) which is an indication of the "natural" weakening of the pandemic for a non-controlled population scenario. These play the same roles as **velocity** and **gravity** respectively in projectile motion. Higher-degree terms e.g. the third-order if present provides departure from projectile-type behavior and may be associated with decay in the projectile dynamics or control in the case of the pandemic.

Using the function notation; $T = f(z)$, κ is given by;

$$\kappa = \frac{f^{II}(z)}{[1+(f^{I}(z))^2]^{3/2}} \tag{7}$$

And using equation 5 in 7;

$$\kappa = \frac{2\eta_2}{[1+(2\eta_2 z+\eta_1)^2]^{3/2}} \tag{8}$$

For small slopes expected for short data length, equation 8 may be approximated as;

$$\kappa = 2\eta_2 \tag{9}$$

So that the peak of the pandemic curve occurs at;

$$z = \frac{-\eta_1}{2\eta_2} \tag{10}$$

Hence at peak period of pandemic without control, the curve contains significant information on both transmissivity and curvature of the pandemic.

In a resistive atmosphere, the drag force F_d on the projectile of mass m and density ρ opposes motion according to the equation;

$$F_d = mg = \frac{1}{2} C_d \rho A v^k \tag{11}$$

Where v, is the velocity, $A$is the projected area of the particle and C_d is the drag coefficient and k=1, 2, 3…defines the relation between drag and velocity for the given problem. A trivial analytical result is possible with any power of n (see e.g. [17], [18]. Considering linear drag (k=1) for a moderate speed projectile, F_d can be expressed according to the equation;

$$F_d(v) = m\frac{dv}{dt} = mg - bv \tag{12}$$

Where $b = \frac{1}{2} C_d \rho A$ is drag constant.

The two component motions are;

$$\frac{dv_x}{dt} = \frac{b}{m} v_x \text{ (Equation of range)} \tag{13}$$

and

$$\frac{dv_y}{dt} = -g - \frac{b}{m} v_y \ (\textit{Equation of height}) \tag{14}$$

In the resistive medium, the velocity v reaches its terminal value V_t("terminal velocity") at which drag on the projectile particle maximizes after a critical time $n\tau$ (n=1, 2, 3, 4…) according to the equation;

$$v = V_t[1 - e^{-t/\tau}] \tag{15}$$

Where $V_t = \frac{m}{b} g$, so that; $\frac{b}{m} = \frac{g}{V_t}$ is the resistive term, and the equation of range becomes;

$$\frac{dv_x}{dt} = -g\frac{v_x}{V_t} \tag{16}$$

The area swept out by the difference between two projectiles in free atmosphere (i) and resistive atmosphere (j) is quantified by integrating equation 16 over the two paths specified by the projectile velocities; v_{ix} and v_{jx}, i.e;

$$\int_{v_{ix}}^{v_{jx}} \frac{dv_x}{v_x} = \int_0^t \frac{-g}{V_t} dt \tag{17}$$

$$[Inv_x]_{vix}^{vjx} = -g\frac{t}{V_t} \tag{18}$$

Or

$$v_{jx} = v_{ix} e^{-\lambda t} \tag{19}$$

The resistance therefore causes exponential decay in the horizontal velocity v_{ix} of amount $\lambda = \frac{g}{V_t}$ on a time scale of $\beta = \lambda^{-1}$ (which is the "projectile decay constant"). The decay results in reduction in the range of the projectile in the resistive atmosphere. Using equation 19, the resistance on the projectile may therefore be quantified from the "projectile decay series";

$$\beta = [(Inv_{ix} - Inv_{jx})/t]^{-1} \tag{20}$$

Following the PMP, a pandemic transmitting in a population without control (g) in pandemic space (z) with transmissivities; η_{gz} and the pandemic under a controlled population (f) with transmissivities; η_{fz} will on the basis of Equation 19 satisfy;

$$\eta_{fz} = \eta_{gz} e^{-\mu t} \tag{21}$$

Where $\mathcal{U} = \mu^{-1}$ is the "pandemic reduction constant" so that the "pandemic reduction series" is;

$$\mathcal{U} = [(In\eta_{gz} - In\eta_{fz}) / t]^{-1} \tag{22}$$

3.0 Implementing the Model for Selected Countries

To implement the framework, we considered COVID-19 countries-data obtained from the World Health Organization (WHO) Corona-virus (COVID-19) Dashboard ([19]) which presented daily counts of COVID-19 cases and deaths worldwide. Twenty countries were selected from a pool of high-burdened countries during the early pandemic period and ensuring spread across continents as follows:

- **North and Sub-Saharan Africa:** Algeria, Ghana, Morocco, Nigeria and South Africa
- **The Americas:** Brazil, Canada, Mexico, Peru and USA,
- **Asia and Western Pacific:** Australia, China, India, Iran and Saudi Arabia
- **Europe and United Kingdom:** United Kingdom, Germany, France, Italy and Spain

We need to derive β and $\mathcal{U}$ for the countries and then examine the agreement between them.

3.1 *Estimating β parameters (i.e v_{ix} and v_{jx}) for the Countries*

To estimate β using equation 20 we need to generate the velocities with and without drag (i.e v_{ix} and v_{jx} respectively). This was done

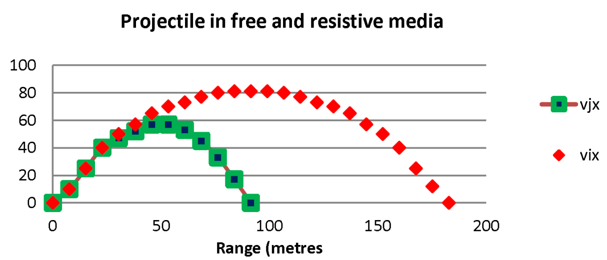

Figure 2

Computer-generated velocities of a projectile in free space (v_{ix}) and under a resistive medium (v_{jx}) using the provided constants. Projectile in resistive medium curves rapidly on reaching terminal velocity compared to projectile in free air

experimentally based on equation 11, using the following arbitrary constants for a model projectile before and after resistance; v = 20m/s, θ = 45°, C_d = 0.5, m = 5kg, ρ = 1.225kg/m^3 and A = 0.25. Figure 2 is a plot of v_{ix} and v_{fx} obtained with these values.

3.2 *Estimating $\mathcal{U}$ Parameters (i.e η_{iz} and η_{fz}) for different countries*

Generating η_{iz}

To generate $\mathcal{U}$, we require the transmissivity without control (η_{iz}) and the transmissivity under control (η_{fz}) for the various countries- η_{iz} are points on the parabolas generated from second-degree polynomials of coefficients η_1 (transmissivity) and η_2 (curvature) fitted over ten weeks of the cumulative cases, commencing from the point of transition to triple or higher digit cases. This for most countries signaled the inception of community transmission of the virus. From equation 10, this period is about the minimum required for reproducing both the transmissivity and curvature characteristics of the early wave for each country (Table 2). In Africa as Table 2 indicates, the transmissivity was lowest compared to other countries (See [20]).).

Generating η_{fz}

The observed pandemic points, η_{fz} representing transmissions under control is expected to be more gradual and therefore were estimated from the one-point moving averages of the weekly means of number of cases of the infection. The early pandemic wave progressed differently in different countries.

Table 2

Transmissivity (η_1) and curvature (η_2) of the generating polynomial for determining the transmissivities without control (η_{iz}) for the listed Countries

Country	Date*	η_1	η_2
Australia	10-03-20	0.408	-0.105
Algeria	**17-03-20**	**0.483**	-0.063
South Africa	**17-03-20**	**0.516**	-0.051
Morocco	**17-03-20**	**0.537**	-0.078
Ghana	**24-03-20**	**0.58**	-0.051
Iran	**24-02-20**	**0.596**	-0.117
Nigeria	**24-03-20**	**0.627**	-0.037
China	13-01-20	0.677	-0.147

AFRICAN COUNTRIES showing lowest transmisivities (Only below Australia)

Contd...

Mexico	17-03-20	0.7	-0.065
India	10-03-20	0.78	-0.058
Canada	10-03-20	0.798	-0.094
Saudi Arabia	10-03-20	0.805	-0.08
UK	3/3/2020	0.813	-0.112
Brazil	10-03-20	0.829	-0.087
France	24-02-20	0.839	-0.141
Germany	24-02-20	0.869	-0.144
Peru	10-03-20	0.941	-0.082
Spain	3/3/2020	1.01	-0.189
Italy	24-02-20	1.079	-0.203
USA	3/3/2020	1.134	-0.124

*Date of commencement of 10-week cumulative count (dd-mm-yy); η_1 -The linear term is the early transmissivity of 10-weeks cumulative count from inception of community spread; η_2 -The quadratic term is the early curvature of 10-weeks cumulative count from inception of community spread

Plots of η_{iz} and η_{fz} for Different Countries

The η_{iz} and η_{fz} curves for the various countries are as shown in Figure 3. The closer the residual of η_{iz} and η_{fz} is to a parabola, the better the pandemic control.

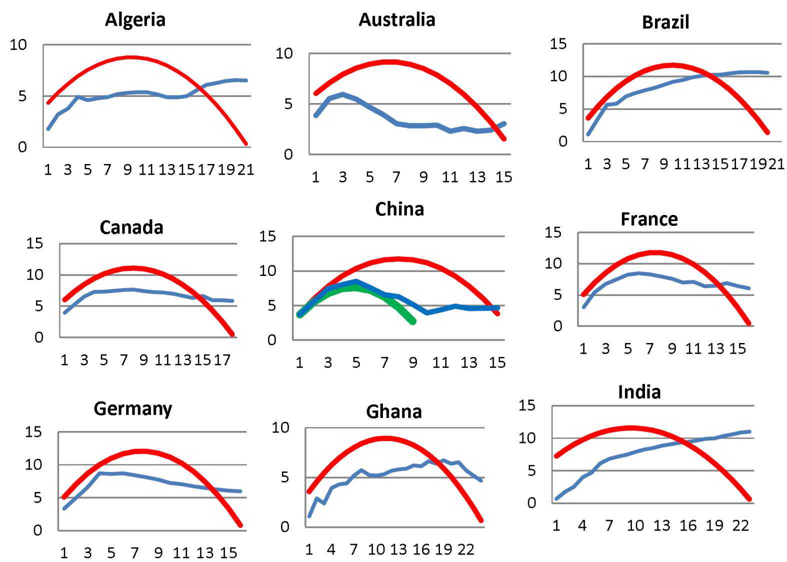

Contd...

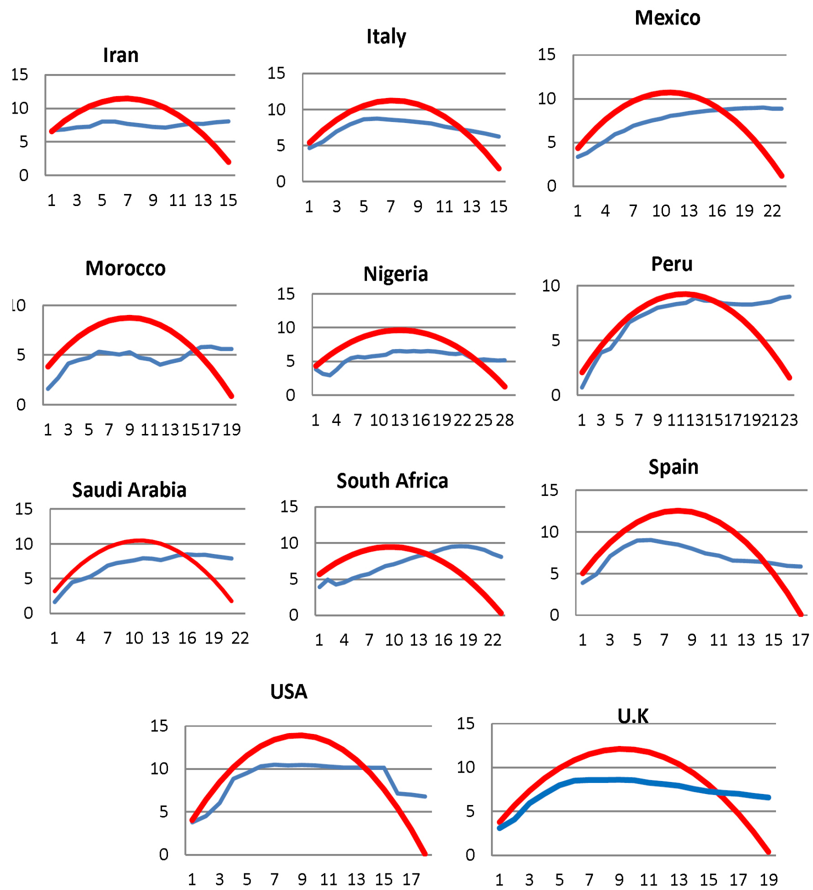

Figure 3

Projected (η_{iz}) and –observed (η_{fz}) transmissions for the countries indicated. The axes and color legends are as indicated in Figures. 4.

The China Example

The curves in Figure 3 indicate (except for China) that compared to the projected transmissions, the observed transmissions do not decay rapidly along a parabolic path which would make the residual of η_{iz} and η_{fz} to include a clear quadratic component (shown for China). These country-curves therefore depart markedly from the projectile model and show less control of the pandemic compared to China. (see expanded plot for China shown in Figure 4).

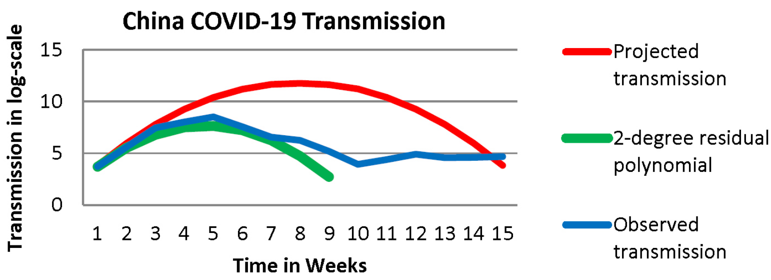

Figure 4

Projected (η_{iz}), observed (η_{fz}) and 2-degree residual plots for China showing close correspondence with projectile model

3.3 *Comparing β and $\mathcal{U}$ using the China Model as Illustration*

Since for a perfect control, we require the polynomials defining β and $\mathcal{U}$ to match for a perfect control, the levels of COVID-19 control by countries, may be assessed by comparing the r-square for β (i.e R_β^2) and the r-square for $\mathcal{U}$ (i.e $R\mu^2$) using the paramerter ε as follows:

$$\varepsilon = R_\beta^2 / R_\mu^2 \tag{23}$$

Following equation 11, the velocity dependence of the drag may be better approximated by a higher power of *v*, hence a polynomial approximation to the exponential function for both the decay and control series may be more appropriate i.e;

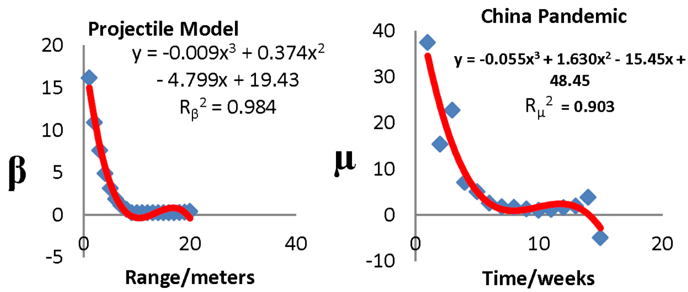

(a) (b)

Figure 5

Plots and fitted 3-degree polynomials for (a) residual of projectile in free and resistive atmosphere (b) residual of China pandemic with and without control

$$e^{\lambda} = \sum_{n=0}^{\infty} \frac{\lambda^n}{n!} = 1 + \lambda + \frac{\lambda^2}{2} + \frac{\lambda^3}{6} + \frac{\lambda^4}{24} \quad (24)$$

Following equation 23, ε =1 for exact projectile-type control or perfect pandemic control and assumes higher values as the control departs from projectile situation. Figure 5 shows plots of β compared with plots of $\mathcal{U}$ for China. For this example $\varepsilon = R_\beta^2/R_\mu^2 = 0.984/0.903 = 1.1$, which is the closest of the cases considered to perfect projectile-type decay synonymous with perfect pandemic control.

Again since ε should translate to a reduction in the cases of transmission compared to the projections under a no-control situation, we may denote by γ the fraction that the pandemic transmission reduces to on account of the control measures, i.e;

$$\gamma = \frac{\langle \exp(\eta_{fz}) \rangle}{\langle \exp(\eta_{gz}) \rangle} \quad (25)$$

With a maximum value of 1, the amount by which the pandemic is reduced using the control measures over the entire period projected for the pandemic is; $\Omega = 1-\gamma$, i.e

$$\Omega = 1 - \frac{\langle \exp(\eta_{fz}) \rangle}{\langle \exp(\eta_{gz}) \rangle} \quad (26)$$

4.0 Results of the ε and γ Evaluation Metrics for the Countries

We present in Table 3, the fit constants for β and $\mathcal{U}$ and the evaluated R^2; as well as the corresponding values of ε and γ for all the countries evaluated. The relationship between ε and γ is plotted in Fig. 6. It is strongly logarithmic (R^2= 0.702) and permits a cluster grouping with some useful outcomes characterizing the levels of performance of countries in controlling the pandemic. Four cluster groups have been delineated over equally spaced values of ε as follows: Cluster 1; ε = 0.0-4.0, Cluster 2; ε = 4.1-8, Cluster 3; ε = 8.1-12 and Cluster 4; ε = 12.1-).

Cluster 1 countries provide the best pandemic control followed by Cluster 2 and then Cluster 3 and lastly Cluster 4.Cluster 1 countries show the least variability of ε with γ and contains the countries; China (ε =1.1), Australia (ε =2.7), Germany (ε =3.1), Canada (ε =3.2), USA (ε =3.2) and UK (ε =3.7) and this cluster is generally associated with reductions in observed transmission periods compared to the projected. Cluster 2 countries are; Italy (ε = 4.8), France (ε = 5), Spain (ε = 5.2), Morroco (ε =

5.2), Nigeria ($\varepsilon = 6.2$), Algeria ($\varepsilon = 6.4$), Brazil ($\varepsilon = 6.9$) and Saudi Arabia ($\varepsilon = 7.1$). Cluster 3 countries are Ghana ($\varepsilon = 8.3$), Peru ($\varepsilon = 10.7$) and Mexico ($\varepsilon = 10.9$). Cluster 4 countries (South Africa with ε =14.9 and India (ε =12.6) are adjudged to have achieved the poorest control under the PAP framework even though India recorded much more reduced transmission than Nigeria, Brazil, and Peru over same period. Hence success under the PAP framework requires reductions in both the transmission intensity and duration of the pandemic. A linear scale plot of ε and γ is shown in Figure 7. The figure shows the occurrence of γ for South Africa and Peru beyond the 1 point mark indicating that both

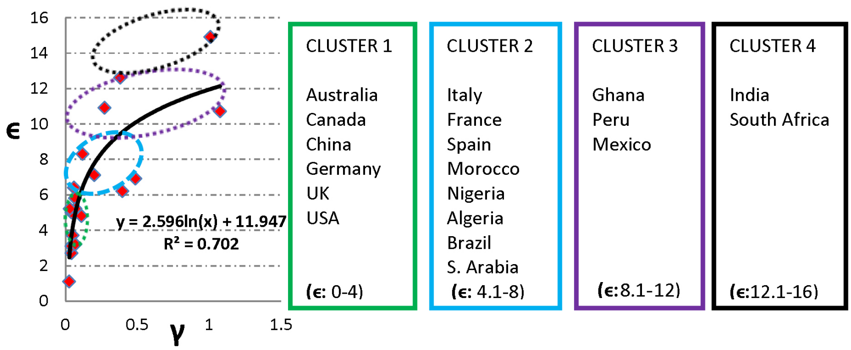

Figure 6

Relationship between the fits ratio (ϵ) and reduction fraction (γ); and the resulting cluster grouping of the countries

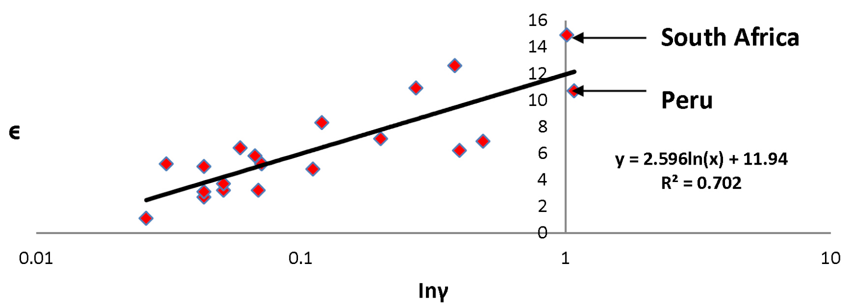

Figure 7

Linear scale plot of the two parameters (ε and γ); South Africa and Peru recorded γ beyond unity threshold indicating that their observed transmission situations got worse than what were projected

countries could not reduce their transmissions below their business-as-usual projections for the period. This raises concerns as to efficiency of the control measures adopted by these countries during the period under examination.

5.0 Benchmarking Country-Control Using the China Example

It is obvious that the circumstances that produced the pandemic control constants for each country are unique for the country. The case of China serves a good illustration. First, considering Figure 5, the largest y-axis intercepts a_0 will be recorded for the best control. The largest residual intercept was for China (a_0 = 48.45). The linear term; a_1, which is partially an indication of "residual transmissivity" is also important. The smallest value was observed for China (a_1 = –15.45). Using the projectile model, the curvature term of the residual, a_2 is the "curve flattening" measure and indicates how rapidly the observed curve decays in comparison with the projectile model-with the magnitude indicating the level of control. The highest value was recorded for China (a_2 = 1.630). The cubic term; a_3 (the "tail" of the residual) estimates the period of observed transmission compared to the projected transmission. A large tail indicates a highly prolonged first wave or an early commencement of the second wave compared to the projected range. China recorded the lowest values (a_3 = –0.055). In all, China's results (R^2 = 0.903; ε =1.1 and γ = 0.026) provide the best fit using the projectile model. It is on record that at the commencement of community transmission of the pandemic in Wuhan, China instituted immediate, comprehensive and population-compliant interventions to counter the pandemic ([16]), which resulted in clear and considerably high departure from the projection. The tail although present is only weak in line with the realistic expectation of non-abrupt end for a pandemic. This indicates that the China control parameters can provide useful benchmarks for appraising pandemic control using the projectile model. One may also notice that although Germany and France recorded similar projected transmissivity and curvature, Germany achieved a Cluster 1 ranking, while France achieved a Cluster 2 ranking on the basis of dissimilar efficiencies of their control measures during the period considered. Countries can therefore interrogate the measures adopted on the basis of these results.

Table 3

Residual fit constants for the projectile (β) and country-pandemics transmissions ($\mathcal{U}$) and the evaluated R², ε and γ

Fit constants	a_0	a_1	a_2	a_3	R^2	ε	Y
Projectile	19.43	-4.799	0.374	-0.009	0.984	1	-
Algeria	1.68	-0.034	0.028	-0.001	0.154	6.4	0.059
Australia	4.49	-0.962	0.096	-0.003	0.37	2.7	0.043
Brazil	-6.106	5.327	-0.684	0.021	0.142	6.9	0.487
Canada	2.305	0.318	-0.017	0	0.306	3.2	0.051
China	**48.45**	**-15.45**	**1.63**	**-0.055**	**0.903**	**1.1**	**0.026**
France	4.053	-0.678	0.134	-0.007	0.195	5	0.043
Germany	1.972	0.864	-0.092	0.001	0.318	3.1	0.043
Ghana	2.973	-0.964	0.145	-0.004	0.118	8.3	0.120
India	-3.686	2.21	-0.203	0.004	0.078	12.6	0.381
Iran	-122.3	80.26	-12.65	0.522	0.171	5.8	0.067
Italy	9.927	-3.494	0.587	-0.027	0.203	4.8	0.111
Mexico	1.707	0.418	0.009	0	0.09	10.9	0.272
Morocco	1.649	0.014	0.023	-0.001	0.188	5.2	0.071
Nigeria	4.047	-0.43	0.05	-0.001	0.158	6.2	0.397
Peru	-42.44	31.42	-4.281	0.134	0.092	10.7	1.076
S.Arabia	-1.313	1.935	-0.196	0.004	0.138	7.1	0.201
S.Africa	0.302	-1.145	0.443	-0.018	0.066	14.9	1.009
Spain	5.078	-0.777	0.113	-0.005	0.191	5.2	0.031
UK	4.529	-0.196	0.03	-0.002	0.263	3.7	0.051
USA	10.44	-1.362	0.089	-0.003	0.305	3.2	0.069

6.0 Socio-Economic Aspects of the Cluster Evaluation and Implications for Africa

The presented framework evaluates the capacity of a country to reduce the disease numbers as well as duration compared to those projected from the initial no-control scenario. It is therefore not dependent on the transmissivity. This point is illustrated in Table 4 which shows that Cluster-1 countries although with the highest average transmissivity $\langle \eta_1 \rangle$ = 0.912, recorded the best control of the pandemic compared to the lower transmissivity countries. Socio-economic factors seemed very apparent in the cluster trends as greater proportion of developed countries appeared in the first cluster and less in the second, third and fourth clusters. The socio-economic link is strengthened in Table 4 using the Human Development Index (HDI) and the Per-Capita Gross Domestic Product (GDP), sourced from the United Nations Development Program data for 2019 (www.undp.org). These data show that both the GDP and the HDI are averagely higher as one moves up the cluster groupings.

Table 4

Ranges of ϵ corresponding to the indicated clusters of Figure 6 and the associated averages of Transmissivity, GDP and HDI

Cluster	ε	$\langle \eta_1 \rangle$	$\langle GDP \rangle$	$\langle HDI \rangle$
cluster 1	0.0-4	0.912	43.71	0.91
cluster 2	4.1-8	0.651	16.77	0.79
cluster 3	8.1-12	0.713	6.43	0.72
cluster 4	12.1-16	0.675	4.13	0.67

It can be adduced that the generally poor GDP of developing countries might have translated to poor palliatives for the population during lock-down, which hampered the sustainability of lockdown in developing countries. The HDI often expressed in terms of illiteracy, unemployment and poor access to electricity would have equally impacted control negatively as people could not perform optimally under lock-down. In most developing countries as found in Africa, significant lock-down could not be achieved because much of the populations had unstable or no employment and limited access to capital. It is notable that countries such as Mexico, Peru, South Africa and India which recorded the poorest control of the early pandemic transmissions as shown in this study later experienced escalation in cases and mutation to new more transmissible variants. This shows that early control of the pandemic is a sure way of preventing deterioration of a pandemic situation. The above results agree strongly with those of Jamison and co-workers as well ([13]) as well as Delis and co-workers [21]) using other ranking methods.

5.0 Conclusions

This work has shown that a mechanical projectile in free space effectively models the parabolic curve that fits the cumulative cases of a pandemic disease in log-scale. Consequently, the dynamics of the projectile under a resistive force can be used to estimate the pandemic under control. This framework has been employed to evaluate the different levels of control of COVID-19 pandemic achieved by 20 selected countries during the first 5 months of the disease. China's early disease trajectory fitted the theoretical projectile best and therefore serves as veritable benchmark for the management of the COVID-19 pandemic and others in future. In addition to governance efficiency, the capacity of a country to control the pandemic has been found to correlate strongly with socio-economic factors and this has huge implication for future management of pandemics in Africa and the rest of the developing world. The framework tracks the performance within a pandemic cycle and can therefore be extended to incorporate more cycles. The evaluation can also be extended to any number of countries.

Acknowledgements

The authors are grateful to World Health Organization for availability of the data on the website.

Conflict of Interests

There are no conflicts of interests declared in the course of this study

References

[1] N. R. Hussein, I. A. Nagid, Z. S. M-Salem, L. A. Almizon, D. H. Musa, and N. Ibrahim, "A sharp increase in the number of COVID-19 cases and case fatality rates after lifting the lockdown in Kurdistan region of Iraq," *Ann. Med. Surg.*, vol. 57, pp. 140-142 (2020).

[2] S. P. Adhikari, S. Meng, Y.-J. Wu, Y.-P. Mao, R.-X. Ye, Q.-Z. Wang, C. Sun, S. S., R. S., H. Raat, and H. Zhou, "Epidemiology, causes, clinical manifestation and diagnosis, prevention and control of coronavirus disease (COVID-19) during the early outbreak period: a scoping review," *Infect. Dis.*, vol. 9, no. 29 (2020).

[3] F. Wu, S. Zhao, B. Yu, Y. M. Chen, W. Wang, Z.-G. Song, L. Y. Lin, C. L. Xie, L. P. Zhan, M. L. Wang, J. A. Zhu, D. R. Yang, C. H. Wu, Y. Z. Zhang, M. P. Liao, Y. J. Shen, Z. J. Liu, W. R. Xie, Y. X. Yang, and X. H. Chen, "A new coronavirus associated with human respiratory disease in China," *Nature*, pp. 1–5, (2020).

[4] J. Lu, G. J. Gu, K. Li, C. Xu, W. Su, Z. Lai, D. Zhou, C. Yu, B. Xu, and Z. Yang, "COVID-19 outbreak associated with air conditioning in restaurant, Guangzhou, China," *Emerg. Infect. Dis.* (2020). [Online]. Available: https://doi.org/10.3201/eid2607.200764.

[5] P. Zhou, X. L. Yang, X. G. Wang, H. S. Hu, J. L. Zhang, L. M. Li, M. M. Chen, Y. X. Chen, Z. S. Li, X. S. Zhan, Z. L. Zhao, X. X. Wang, S. Q. Guo, Y. Y. Chen, L. W. Zhou, J. L. Chen, J. J. Wei, W. Li, X. L. Wu, D. Y. Xu, Y. Q. Zhang, W. L. Hu, and X. X. Jiang, "Discovery of a novel coronavirus associated with the recent pneumonia outbreak in humans and its potential bat origin," *Nature*, vol. 579, pp. 210–273, (2020).

[6] CDC, "COVID-19 responses," Centers for Disease Control and Prevention. [Online]. Available: https://www.cdc.gov/coronavirus/2019-ncov/about/transmission.html. [Accessed: Jan. 2020].

[7] H. A. Rothan and S. N. Byrareddy, "The epidemiology and pathogenesis of coronavirus disease (COVID-19) outbreak," *J. Autoimmun.*, vol. 109, p. 102433 (2020).

[8] National Center for Immunization and Respiratory Diseases (NCIRD), "SARS-CoV-2 variant classifications and definitions," CDC (2021). [Online]. Available: https://www.cdc.gov/coronavirus/2019-ncov/variants/variant-info.html.

[9] R. S. Mariano and S. Ozmucur, "Fighting COVID-19: Performance of countries in the first half of 2020," PIER Working Paper 20-040 (2020).

[10] V. Singh, R. C. Poonia, S. Kumar, P. Dass, P. Agarwal, V. Bhatnagar, and L. Raja, "Prediction of COVID-19 coronavirus pandemic based on time series data using support vector machine," *J. Discrete Math. Sci. Cryptogr.* (2020). [Online]. Available: https://doi.org/10.1080/09720529.2020.1784535.

[11] N. Hau, L. Geyrhofer, A. Londei, E. Dervic, A. Desvars-Larrive, V. Loreto, B. Pinior, S. Thurner, and P. Klimek, "Ranking the effectiveness of worldwide COVID-19 government interventions," *Nature Hum. Behav.*, vol. 4, pp. 1303–1312 (2020). [Online]. Available: www.nature.com/nathumbehav.

[12] V. Bhatnagar, R. C. Poonia, P. Nagar, S. Kumar, V. Singh, L. Raja, and P. Dass, "Descriptive analysis of COVID-19 patients in the context of India," *J. Interdiscip. Math.*, vol. 24, no. 3, pp. 489-504 (2021). [Online]. Available: https://doi.org/10.1080/09720502.2020.1761635.

[13] D. T. Jamison, L. J. Lau, K. B. Wu, Y. Xiong, and V. Country, "Performance against COVID-19: Rankings for 35 countries," BMJ Global Health, vol. 5, p. e003047 (2020). [Online]. Available: https://doi.org/10.1136.

[14] R. Alguliyev, R. Aliguliyev, and F. Yusifov, "Graph modeling for tracking the COVID-19 pandemic spread," *Infect. Dis. Model.*, vol. 6, pp. 112-122 (2021).

[15] H. Yan, Y. Zhu, J. Gu, Y. Huang, H. Sun, X. Zhang, Y. Wang, Y. Qiu, and S. Xi Chen, "Better strategies for containing COVID-19 pandemic: A study of 25 countries via a vSIADR model," Proc. R. Soc. A, vol. 476, p. 20200440 (2021). [Online]. Available: https://doi.org/10.1098/rspa.2020.0440.

[16] X. Chen and B. Yu, "First two months of the 2019 Coronavirus Disease (COVID-19) epidemic in China: Real-time surveillance and evaluation with a second derivative model," *Global Health Res. Policy*, vol. 5, Article no. 7 (2020).

[17] E. N. Miranda, S. Nikolskaya, and R. Riba, "Minimum and terminal velocities in projectile motion," Rev. Bras. Ens. Fís., vol. 26, no. 2, pp. 125-127 (2004). [Online]. Available: www.sbfisica.org.br.

[18] Y. P. Hu, Y. J. Zhao, M. Y. Guo, and Z. Zheng, "Analysis of linear resisted projectile motion using the Lambert W function," *Acta Mech.*, vol. 223, pp. 441–447 (2012). [Online]. Available: https://doi.org/10.1007/s00707-011-0571-2.

[19] World Health Organization, "COVID-19 Dashboard," (2020). [Online]. Available: https://covid19.who.int.

[20] S. J. Salyer, J. Maeda, S. Sembuche, Y. Kebede, A. Tshangela, M. Moussif, C. Ihekweazu, N. Mayet, E. Abate, A. Ogwell Ouma, and J. Nkengasong, "The first and second waves of the COVID-19 pandemic in Africa: A cross-sectional study," Lancet, vol. 397 (2021).

[21] M. D. Delis, M. Iosifidi, and M. Tasiou, "Efficiency of government policy during the COVID-19 pandemic," MPRA Paper No. 107046 (2021). [Online]. Available: https://mpra.ub.uni-muenchen.de/107046/.

Received August, 2022